Journal of Hazardous Materials xxx (xxxx) xxxx

Contents lists available at ScienceDirect

Journal of Hazardous Materials

journal homepage: www.elsevier.com/locate/jhazmat

Non-target screening reveals the mechanisms responsible for the antagonistic inhibiting effect of the biocides DBNPA and glutaraldehyde on benzoic acid biodegradation

Thomas V. Wagner[a,b,*], Rick Helmus[a], Silvana Quiton Tapia[b], Huub H.M. Rijnaarts[b], Pim de Voogt[a,c], Alette A.M. Langenhoff[b], John R. Parsons[a]

[a] Institute for Biodiversity and Ecosystem Dynamics (IBED), University of Amsterdam, P.O. Box 94248, 1092 GE, Amsterdam, the Netherlands
[b] Department of Environmental Technology, Wageningen University, P.O. Box 17, 6700 EV, Wageningen, the Netherlands
[c] KWR Water Research Institute, Chemical Water Quality and Health, P.O. Box 1072, 3430 BB, Nieuwegein, the Netherlands

GRAPHICAL ABSTRACT

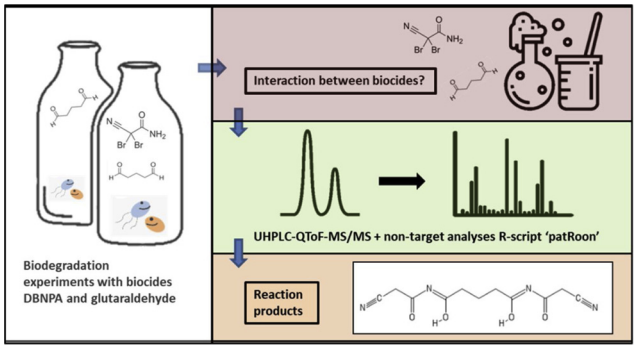

ARTICLE INFO

Editor: R. Debora

Keywords:
Constructed wetlands
Non-target screening
Biocides
Cooling tower water

ABSTRACT

The desalination and reuse of discharged cooling tower water (CTW) as feed water for the cooling tower could lower the industrial fresh water withdrawal. A potential pre-treatment method before CTW desalination is the use of constructed wetlands (CWs). Biodegradation is an important removal mechanism in CWs. In the present study, the impact of the biocides 2,2-dibromo-2-cyanoacetamide (DBNPA) and glutaraldehyde on the biodegradation process by CW microorganisms was quantified in batch experiments in which benzoic acid was incubated with realistic CTW biocide concentrations. DBNPA had a stronger negative impact on the biodegradation than glutaraldehyde. The combination of DBNPA and glutaraldehyde had a lower impact on the biodegradation than DBNPA alone. UHPLC-qTOF-MS/MS non-target screening combined with data-analysis script 'patRoon' revealed two mechanisms behind this low impact. Firstly, the presence of glutaraldehyde resulted in increased DBNPA transformation to the less toxic transformation product 2-bromo-2-cyanoacetamide (MBNPA) and newly discovered 2,2-dibromopropanediamide. Secondly, the interaction between glutaraldehyde and DBNPA resulted in the formation of new products that were less toxic than DBNPA. The environmental fate and toxicity of these products are still unknown. Nevertheless, their formation can have important implications for the simultaneous use of the biocides DBNPA and glutaraldehyde for a wide array of applications.

* Corresponding author at: Department of Environmental Technology, Wageningen University, P.O. Box 17, 6700 EV Wageningen, the Netherlands.
E-mail addresses: thomas.wagner@wur.nl, t.v.wagner@uva.nl (T.V. Wagner).

https://doi.org/10.1016/j.jhazmat.2019.121661
Received 8 August 2019; Received in revised form 5 November 2019; Accepted 9 November 2019
0304-3894/

1. Introduction

The industrial water sector is responsible for approximately 25 % of the yearly global fresh water withdrawal, of which more than 75 % is withdrawn in industrialized countries (FAO, 2016). In these countries, the uptake of fresh water for cooling processes accounts for a substantial part of the total industrial fresh water uptake (Macknick et al., 2012; Zhang et al., 2016). After its use, the water used for the cooling process is mostly discharged in nearby water bodies. The reuse of discharged cooling tower water (CTW) in the cooling tower itself could help to significantly mitigate future fresh water scarcity problems caused by industrial fresh water withdrawal.

Discharged CTW has a moderate electric conductivity (EC) of 1500 − 4500 mS/cm (Altman et al., 2012; Löwenberg et al., 2015) as result of the evaporative cooling process, while an EC of < 1000 ms/cm is typically required for reuse in cooling towers (Groot et al., 2015). Hence, the reuse of CTW requires its physico-chemical desalination, and an overview of appropriate physico-chemical desalination technologies for CTW is provided in Pan et al. (2018). However, physico-chemical desalination techniques are hampered by chemicals present in CTW, which can for instance lead to fouling of reverse osmosis membranes (Wagner et al., 2018). The chemicals in CTW consist of deliberately added conditioning chemicals, such as antiscalants, corrosion inhibitors and biocides. These chemicals maintain optimal cooling tower functioning, but need to be removed prior to physico-chemical desalination and reuse of CTW.

A possible method to remove these chemicals from discharged CTW is the use of constructed wetlands (CWs). CWs are man-made wetland systems that treat waste water using natural contaminant removal mechanisms. The main removal mechanisms in CWs are aerobic and anaerobic biodegradation, photo-degradation, adsorption to the CW substrate and plant uptake and degradation (Imfeld et al., 2009; Garcia et al., 2010; Wagner et al., 2020). The dominating removal mechanism in a CW is determined by its water flow configuration (He et al., 2018; Wagner et al., 2018). Surface flow CWs facilitate photodegradation and biodegradation (Jasper et al., 2014), while adsorption, biodegradation and plant uptake are important removal mechanisms in planted subsurface flow CWs (Hijosa-Valsero et al., 2016). By combining CWs with different water flow configurations in so-called hybrid-CWs, multiple removal mechanisms can be used to achieve a higher removal of contaminants (Avila et al., 2015).

Biodegradation is an important removal mechanism in all potential CW configurations of the hybrid-CW. The biodegradation in a CW is influenced by various factors, such as the temperature, redox conditions and the presence of vegetation (Wagner et al., 2018). A potential impediment for biodegradation in a CW is the input of water containing toxic compounds that inhibit or significantly reduce the microbial activity. Biocides are an example of such toxic compounds, which are used in cooling towers to prevent microbial growth. Biocides, such as glutaraldehyde and 2,2-dibromo-3-nitrilopropionamide (DBNPA), can have a negative effect on the microbial activity in sediment (McLaughlin et al., 2016; Rogers et al., 2017) and this effect might also be observed in a CW.

Glutaraldehyde and DBNPA are among the most frequently used biocides in cooling towers. They are also used in other processes, such as hydraulic fracturing (Leung, 2001a; Kahrilas et al., 2015; Faber et al., 2017). The biocidal functioning of glutaraldehyde is the result of the aldehyde functional groups that react with amines and thiols at the microbial cell membranes, disrupting proper cell functioning (Russell, 2003). DBNPA similarly reacts with the thiol groups at the cell wall of microorganisms (Klaine et al., 1996; Bertheas et al., 2009). In addition, the biocidal effect of DBNPA is increased by the release of bromine ions (Kahrilas et al., 2015) and the formation of various toxic brominated transformation products (TPs) (Mayes et al., 1985).

The objective of this study was to quantify the impact of glutaraldehyde and DBNPA on the aerobic biodegradation potential in a CW. This impact was quantified by testing the effect of different biocide concentrations on the biodegradation of the corrosion inhibitor benzoic acid in batch experiments. In addition, the impact of the simultaneous use of both biocides was tested because of their presumed synergistic toxic effect to microorganisms (Ganzer et al., 2002). However, preliminary *Daphnia magna* ecotoxicity experiments in our laboratory (unpublished results) revealed that the combination of the biocides showed an antagonistic toxic effect. We hypothesized that this was due to interaction between the two biocides. To confirm this interaction, UHPLC-qTOF/MS combined with the non-target data analysis R-package 'patRoon' was used for the screening and identification of transformation- and reaction products of DBNPA and glutaraldehyde.

2. Materials & methods

2.1. Chemicals

The chemicals used and their suppliers are provided in the Supplementary Info (SI) (Text S1).

2.2. Impact of biocides on benzoic acid biodegradation

2.2.1. Experimental set-up

Aerobic benzoic acid biodegradation experiments by a CW inoculum were performed in triplicate in 250 mL serum bottles closed with butyl rubber stoppers perforated with a needle to maintain aerobic conditions. The bottles were covered with aluminium foil to prevent photodegradation and incubated whilst shaking (120 rpm) at 20 °C. A 1:100 (v:v) ratio of inoculum / 50 mM phosphate based mineral medium based on de Wilt et al. (2018) was used in a total volume of 60 mL. The pH in all experiments was monitored with a PHM-210 (Hach, the Netherlands) and remained stable between 6.5 and 7 during all experiments.

A microbial inoculum was obtained from the sediment of a mature surface flow CW planted with *Phragmites australis* located in Hapert, the Netherlands (51.37 N ; 5.23E), which is functioning as a tertiary treatment step after conventional waste water treatment. The inoculum was stored at 4 °C until use and before use, it was sieved at 2 mm to remove any remaining plant fragments.

Biotic degradation experiments were performed with 50 mg/L benzoic acid in the presence of 0, 0.5, 1, 2.5 or 5 mg/L DBNPA, glutaraldehyde or both biocides together. The benzoic acid and biocide concentrations fall within the typical concentrations for CTW. An experiment with 0 mg/L of the biocides was included in each experiment to assess the variability in the ability of the inoculum to degrade benzoic acid. The fate of glutaraldehyde and DBNPA themselves was tested in similar batch experiments.

Abiotic controls were performed in serum bottles with similar content as the biotic experiments. The serum bottles were closed with butyl rubber stoppers and aluminium crimp caps. The microbial activity was stopped by autoclaving the serum bottle including the inoculum at 120 °C for 20 min followed by the addition of NaN_3 (2 mM), after which the benzoic acid and biocides were added.

Samples of 1.5 mL were taken from the serum bottles at t (h) 0, 8, 24, 30, 32, 50, 56, 72, 80, 96, 168, 173, 214 and 450. These samples were centrifuged at 10.000 rpm for 10 min, filtered over a 0.2 µm polyethersulfone filter, acidified with 1 % (v:v) acetic acid and stored in 1.5 mL glass LC vials at -20 °C until analysis.

2.2.2. Benzoic acid and glutaraldehyde analysis

Benzoic acid was quantified by HPLC-DAD as described in the SI (Text S2). Glutaraldehyde was quantified by colorimetry as described in the SI (Text S3).

2.2.3. Benzoic acid $BioT_{50}$, $BioT_{10}$ and $BioT_{90\text{-}10}$ calculation

The time to reach 50 % ($BioT_{50}$) and 10 % ($BioT_{10}$) of benzoic acid

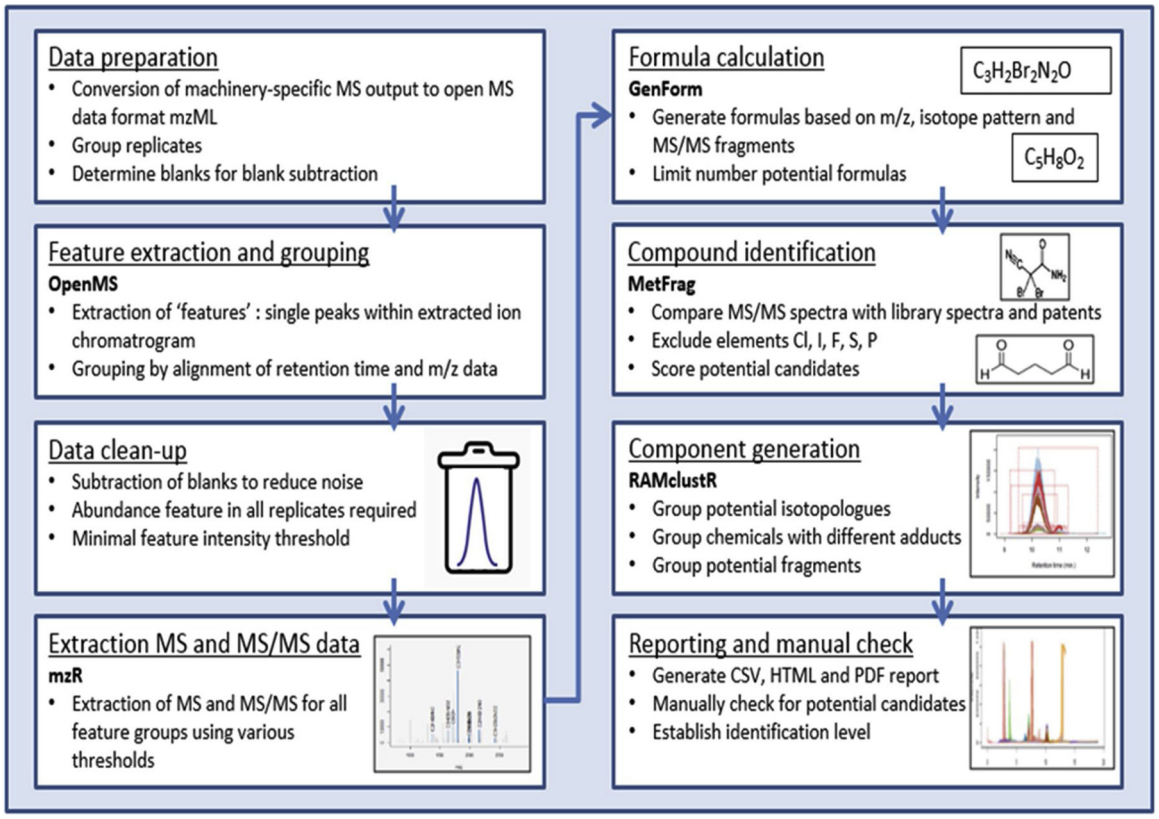

Fig. 1. Workflow for non-target data analysis. Workflow-steps are underlined and accompanying software packages are displayed in bold.

removal and the time to go from 10 % to 90 % of benzoic acid removal ($BioT_{90\text{-}10}$) was determined by performing non-linear regression in SPSS (IBM Statistics, Version 24.0, 2016). An adapted version of a logistic dose response curve proposed by Haanstra et al. (1985) and described by Eq. 1 was fitted to the experimental data:

$$\left(\frac{C_t}{C_0}\right)(t) = \frac{c}{1 + e^{b(\log_{10}x - \log_{10}a)}} \quad (1)$$

In this equation, C_t/C_0 is the residual fraction of benzoic acid in % at time t, x is time t in hours, c is the starting fraction of benzoic acid, which is always 100 %, b is the slope of the curve, with a higher b representing a higher removal rate, and a is the estimated $BioT_{50}$ of benzoic acid.

2.3. Formation of biocide transformation- and reaction products

2.3.1. Experimental set-up

To determine transformation and reaction products of DBNPA and glutaraldehyde, serum bottles of 125 mL closed with butyl rubber stoppers were used, covered with aluminium foil and incubated at 20 °C whilst shaken (120 rpm). The bottles were filled with 1 mg/L DBNPA (D), 1 mg/L glutaraldehyde (G) or 1 mg/L DBNPA + 1 mg/L glutaraldehyde (DG) in ultra-pure (UP) water. To check for interaction between the chemicals and CW sediment, a similar experiment was performed in UP-water including the CW inoculum (CW) with a similar inoculum/medium ratio as in the biodegradation experiments described in paragraph 2.2.1. A UP blank and UP + CW blank without DBNPA, glutaraldehyde or the combination of both was used to prevent false identification of potential reaction products. See Table S1 for an overview of all samples and corresponding sample coding. All experiments were performed in triplicate. Samples of 1 mL were taken at three time points corresponding to 1, 48 and 96 h for UHPLC-q-ToF-MS/MS analysis to monitor the behaviour of potential products over time. These samples were filtered over 0.2 µm polyethersulfone filters and analysed immediately as described in 2.3.2.

2.3.2. Structural elucidation of transformation- and reaction products

UHPLC-q-ToF-MS/MS analyses for non-target screening were performed on a Nexera UHPLC system (Shimadzu, Den Bosch, the Netherlands) coupled to a maXis 4 G high resolution q-TOF-MS/MS upgraded with a HD collision cell and equipped with an ESI source (Bruker Daltonics, Wormer, the Netherlands). Liquid chromatography was performed by a slightly modified version of a method developed by Albergamo et al. (2018). In short, separation of a 20 µl sample was achieved with a core-shell Kinetex biphenyl column (100 × 2.1 mm, 2.6 µm particle size and 100 Å pore size) (Phenomenex, Utrecht, the Netherlands) and the mobile phase consisted of solution A: ultrapure water with acetic acid (0.05 % v:v) and solution B : methanol. A flow rate of 0.2 mL/min was used with a 19-min gradient elution method starting at 0 % B which increased linearly to 100 % B between min 1 and 12. It was maintained at 100 % B for 6 min, after which it decreased to the initial 0 % B in 1 min. The system was then allowed to re-equilibrate for 7 min before the next sample was injected. Prior to each injection, a 50 µM sodium acetate solution in H_2O:MeOH (1:1 v:v) was introduced automatically for recalibration of the system. The column oven was kept at 40 °C. MS and MS/MS were acquired with positive and negative ESI in separate runs with a resolving power typically of 30,000–60,000 FWHM.

2.3.3. Non-target screening data processing workflow

UHPLC-qTOF-MS/MS data was processed in the R programming language (R Core Team, 2013) using an in-house developed R package ('patRoon', Helmus, 2018). The 'patRoon' package provides a common interface to various software solutions that are typically used to implement workflows for mass spectrometry based non-target analysis. Further details about the different software tools can be found at https://github.com/rickhelmus/patRoon. The 'patRoon' workflow for

this experiment is displayed in Fig. 1. The corresponding full R-script that is generated as result of using the 'patRoon' workflow (Text S4) and a more detailed explanation of the workflow (Text S5) are provided in the SI. Two different scripts were used, one for positive and one for negative ionization measurements.

The non-target screening resulted in 25,241 features groups with positive ionization and 6865 feature groups for negative ionization. Prioritization by the filter criteria of the 'patRoon' workflow (Text S5) resulted in 173 feature groups for positive ionization. These feature groups were clustered by RAMClustR in 37 components that contained 124 features groups in total, leaving 49 non-associated feature groups. Prioritization of the feature groups obtained with negative ionization resulted in 80 feature groups, clustered in 18 components that contained 67 feature groups.

3. Results & discussion

3.1. Biodegradation of benzoic acid

The impact of different concentrations of glutaraldehyde and DBNPA on the biodegradation of benzoic acid was tested in batch biodegradation experiments. The $BioT_{50}$, $BioT_{10}$ and $BioT_{90\text{-}10}$ of benzoic acid were used to quantify the required time for 50 % biodegradation ($BioT_{50}$), the lag phase ($BioT_{10}$), and the required time for 90 % biodegradation after the lag phase ($BioT_{90\text{-}10}$) (Table 1).

In the benzoic acid removal experiments without biocides, a lag phase of 22.1–28.5 h (Table 1) occurred, where no removal was observed as evidenced by the $BioT_{10}$. Subsequently, the $BioT_{90\text{-}10}$ showed that 90 % of the benzoic acid was removed within the following 3–5.1 h. An average $BioT_{50}$ of 26.7 h was calculated for all benzoic acid experiments without biocides (Fig. S1). Benzoic acid was removed in the biotic experiments, whereas the abiotic controls that were used to quantify abiotic removal mechanisms showed no removal of benzoic acid (Fig. S1), indicating that the observed removal could be attributed to biodegradation. The CW inoculum was able to biodegrade 90 % of the benzoic acid in 29.3 h. This corresponds with conventional hydraulic retention times (HRT) of CWs, which are generally between 1 and 3 d. Hence, complete biodegradation of the corrosion inhibitor benzoic acid in CTW can be expected in a CW. Consequently, benzoic acid is a suitable proxy to determine the impact of biocides on the biodegradation potential of CW microorganisms.

3.2. The impact of biocides on the biodegradation of benzoic acid

3.2.1. Glutaraldehyde

Increasing concentrations of glutaraldehyde resulted in an increased benzoic acid $BioT_{50}$ (Table 1) (Fig. S2). No abiotic removal of benzoic acid was observed (data not shown), indicating that biodegradation was responsible for the benzoic acid removal. The $BioT_{50}$ mainly increased as result of a prolonged lag-phase after the addition of the glutaraldehyde as evidenced by the increasing $BioT_{10}$. Additionally, the $BioT_{90\text{-}10}$ showed an increasing trend with increasing concentrations of glutaraldehyde. The addition of 5 mg/L of glutaraldehyde, which is ten times lower than used in common cooling tower application (IPCS INCHEM, 2005), increased the required time for 90 % benzoic acid degradation from 29.3 h to 68 h. This reduction in microbial activity is potentially problematic for CWs with low HRTs.

The biodegradation inhibition potential of glutaraldehyde is similar to that reported in earlier studies. Rogers et al. (2017) studied the impact of glutaraldehyde on the biodegradation of hydraulic fracturing chemicals by an aquifer sediment inoculum and found that a glutaraldehyde concentration of 5 mg/L reduced the biodegradation rate, but did not completely inhibit the activity of microorganisms. However, a glutaraldehyde concentration of 50 mg/L and 100 mg/L completely inhibited biodegradation (Rogers et al., 2017). This was also observed in a study by McLaughlin et al. (2016), where 250 mg/L of glutaraldehyde inhibited the biodegradation of the surfactant polyethyleneglycol by an agricultural topsoil inoculum. Hence, higher concentrations of glutaraldehyde than those used in this study and still realistic for CTW, could completely inhibit the biodegradation in a CW.

Glutaraldehyde was quickly removed in both our biotic and abiotic glutaraldehyde removal experiments (Fig. S3). Glutaraldehyde most likely reacted with the membranes of the living microorganisms in the biotic experiments (Russell, 2003), while it also sorbed to dead biomass in the abiotic controls (Leung, 2001a), resulting in decreased glutaraldehyde concentrations. Glutaraldehyde also sorbed to the functional groups of organic matter in a similar way as it does with the functional groups on the membrane of target organisms (McLaughlin et al., 2016), resulting in additional removal of glutaraldehyde from the water phase. Furthermore, abiotic glutaraldehyde removal can occur through hydrolysis and autopolymerisation of the glutaraldehyde (Leung, 2001b). These different abiotic removal pathways could mitigate the negative effect of glutaraldehyde on the microbial activity in a CW. In addition, microorganisms can genetically adapt to the presence of glutaraldehyde (Vikram et al., 2014, 2015; Campa et al., 2018), resulting in an increased glutaraldehyde tolerance and a potentially lower impact of glutaraldehyde on the biodegradation in the CW.

3.2.2. DBNPA

The negative impact of DBNPA on the biodegradation of benzoic acid is stronger than that of glutaraldehyde (Table 1) (Fig. S4). The addition of 0.5 mg/L of DBNPA increased the $BioT_{50}$ of benzoic acid from 26.7 h to 57.9 h. This removal was biological, since no abiotic benzoic acid removal was observed (data not shown). Similar to glutaraldehyde, the increased $BioT_{50}$ is mainly the result of an increased lag-phase after the addition of DBNPA. However, the $BioT_{90\text{-}10}$ also significantly increased after the addition of 2.5 mg/L of DBNPA. No biodegradation was observed within 450 h at a concentration of 5 mg/L of DBNPA (Table 1). This suggests that the biodegradation in a CW would be completely inhibited with this realistic CTW DBNPA concentration, which would negatively impact the CTW pre-treatment efficiency and subsequent CTW desalination. However, DBNPA is very unstable when in solution. The slightly basic pH of CTW (Wagner et al., 2018) could increase the abiotic DBNPA degradation rate (Blanchard et al., 1987). DBNPA also degrades rapidly under UV-light (Exner et al., 1973; Blanchard et al., 1987), a process that could occur in surface flow

Table 1
Biodegradation characteristics of benzoic acid in the presence of different concentrations of DBNPA and glutaraldehyde.

	Glutaraldehyde			DBNPA			Glutaraldehyde + DBNPA		
	$BioT_{50}$ (h)	$BioT_{10}$ (h)	$BioT_{90\text{-}10}$ (h)	$BioT_{50}$ (h)	$BioT_{10}$ (h)	$BioT_{90\text{-}10}$ (h)	$BioT_{50}$ (h)	$BioT_{10}$ (h)	$BioT_{90\text{-}10}$ (h)
0 mg/L	24.3	22.7	3.0	31.0	28.5	5.1	24.0	22.1	5.0
0.5 mg/L	28.3	26.5	3.6	57.9	53.4	9.3	36.7	34.1	5.5
1 mg/L	31.8	28.7	6.6	76.7	70.3	13.4	47.0	44.1	6.0
2.5 mg/L	34.8	30.9	8.2	158.7	133.3	55.9	48.8	42.1	11.1
5 mg/L	57.4	51.9	11.6	> 450	> 450	–	84.8	77.8	14.9

Table 2
Transformation products formed as a result of the direct transformation of DBNPA and the interaction between DBNPA and glutaraldehyde.

TP#[a]	*m/z* (ionization mode)	Detected adduct	RT[b] (min)	Molecular formula and name	PPM error	Level[c]	Sample[d]
–	240.8609 (-)	$[M+H]^+$	7.6	$C_3H_2Br_2N_2O$ DBNPA	−0.4	1	D-UP-1 D-CW-1 D-UP-48 D-CW-48 D-UP-96 D-CW-96
1	162.9473 (+) 160.9354 (-)	$[M+H]^+$ [M-H]-	2.8	$C_3H_3BrN_2O$ MBNPA	0.7	1	D-UP-1 D-CW-1 D-UP-48 D-CW-48 D-UP-96 D-CW-96
2	258.8714 (+)	$[M+H]^+$	4.9	$C_3H_4Br_2N_2O_2$ 2,2-dibromopropanediamide	−0.9	1	DG-UP-1 DG-UP-48 DG-CW-48 D-CW-48 DG-UP-96 DG-CW-96 D-UP-96 D-CW-96
3	183.0760 (+)	$[M+H]^+$	7.1	$C_8H_{10}N_2O_3$	1.5	4	DG-CW-1 DG-UP-48 DG-CW-48 DG-UP-96 DG-CW-96
4	263.0783 (+)	[M-H]-	7.8	$C_{11}H_{12}N_4O_4$	−2.2	4	DG-CW-48 DG-CW-96
5	280.0292 (+)	$[M+H]^+$	8.1	$C_8H_{14}N_3O_3Br$	−0.6	3	DG-CW-96
6			8.3		–		
7			8.9		1.0		

Abbreviations: [a]Transformation product number; [b]Retention time; [c]Identification confidence level according to Schymanski et al., 2014; [d]Sample occurrence.

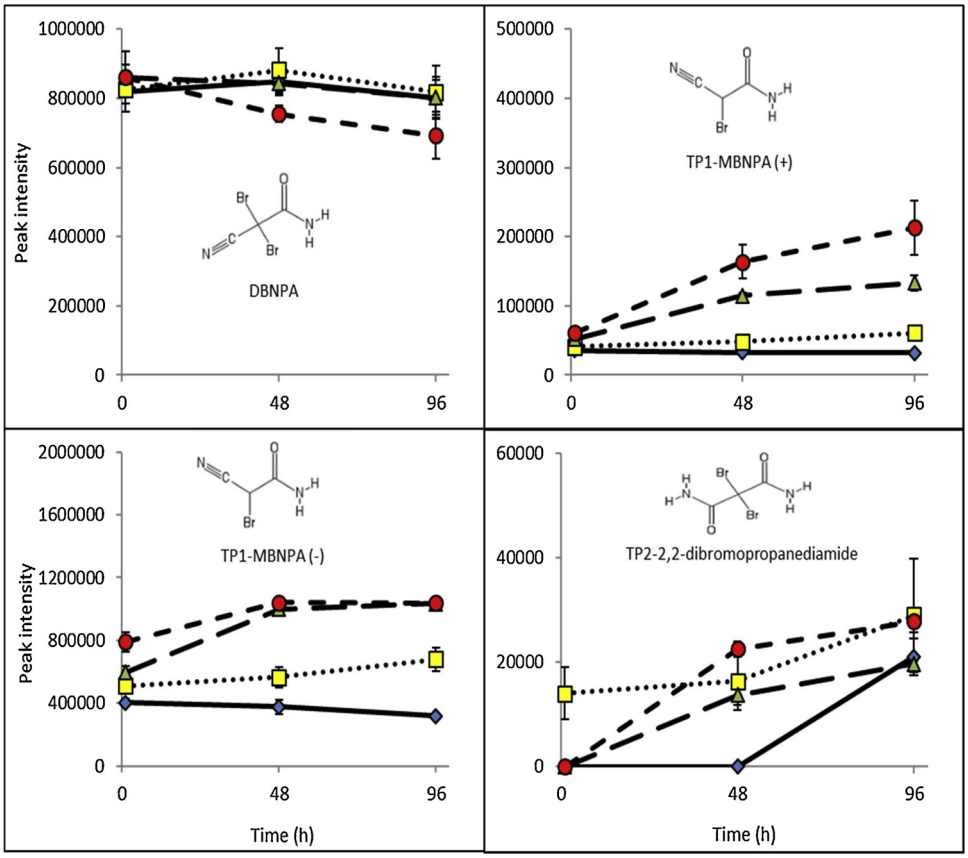

Fig. 2. The peak intensity of DBNPA and DBNPA transformation products over time. A distinction is made between samples in: UP-water (blue diamond); UP-water + glutaraldehyde (yellow square); CW-matrix (green triangle); CW-matrix + glutaraldehyde (red circle).

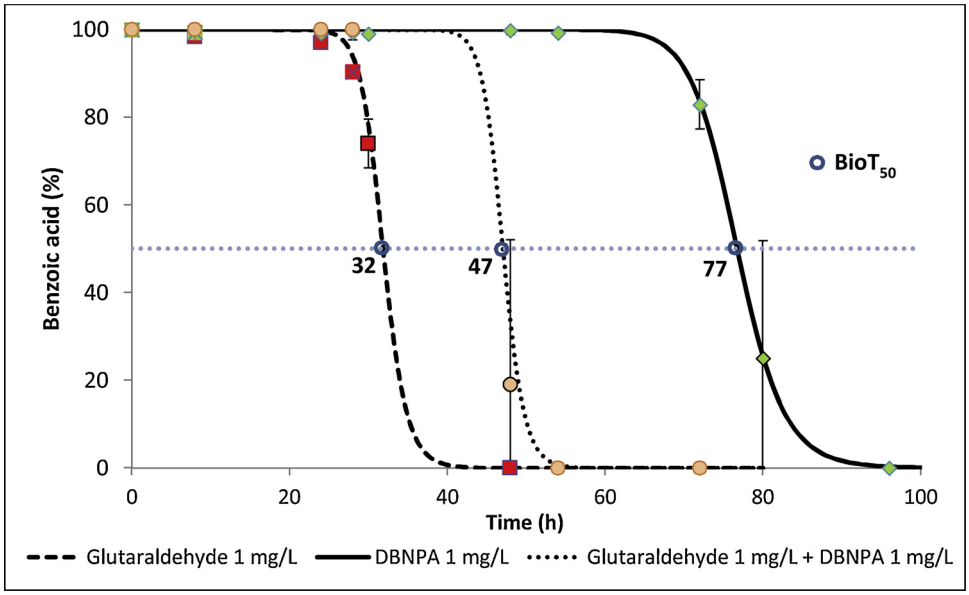

Fig. 3. Residual benzoic acid in the presence of 1 mg/L glutaraldehyde (red squares), 1 mg/L DBNPA (green diamonds) and 1 mg/L glutaraldehyde + 1 mg/L DBNPA (orange circle) over time and the fit of the non-linear time-residual benzoic acid relationship.

CWs. Hence, a hybrid-CW design which promotes the abiotic removal of DBNPA and glutaraldehyde in its first part could mitigate their negative impact on the microbial activity in later stages. However, the abiotic degradation of DBNPA has been shown to result in TPs that are more toxic than the parent compound itself, such as dibromoacetonitrile (Blanchard et al., 1987). Therefore, we studied the formation of DBNPA TPs using the non-target screening workflow depicted in Fig. 1. DBNPA and two brominated TPs were identified (Table 2). DBNPA (Text S6) itself was identified with positive ionization and was present in the samples with only DBNPA (D-samples) as well as in the samples with DBNPA and glutaraldehyde (DG-samples). In addition, DBNPA was present in both the ultra-pure water matrix (UP-matrix) and the UP + constructed wetland material matrix (CW-matrix) (Table 2; Fig. 2A). However, DBNPA could not be quantified due to its instability, even after sample pre-treatment as described in Oetjen et al. (2017).

The first transformation product, TP1, 2-bromo-2-cyanoacetamide (MBNPA) (Table 2; Text S7), was identified by retention time and fragmentation alignment with a commercially available standard in both positive and negative ionization mode. MBNPA is formed after the loss of one bromine ion (Exner et al., 1975). TP1-MBNPA was observed in both the UP-matrix and CW-matrix at the different experimental time points (Fig. 2B; C). In the UP-matrix, the peak intensity of TP1-MBNPA slightly decreased after 96 h in the D-samples, while the presence of glutaraldehyde in the DG-samples led to an increase in peak intensity after 96 h (Fig. 2B; C), indicating that more TP1-MBNPA was produced in the presence of glutaraldehyde. The peak intensity of TP1-MBNPA was higher and increased more over time in the CW-matrix, which was even more pronounced in the samples containing glutaraldehyde (DG-CW) (Fig. 2B; C). This is likely the result of the interaction of DBNPA with organic matter of the CW-matrix, which is in accordance with the study of Blanchard et al. (1987), who found higher MBNPA production in lake water containing 6 mg/L of total organic carbon (TOC) than in ultra-pure water. The highest production of TP1-MBNPA in the DG-CW samples corresponds with the highest decrease of the peak intensity of DBNPA (Fig. 2A). This implies that the transformation of DBNPA and the release of bromine ions is significantly impacted by the composition of the water matrix, and that glutaraldehyde appears to directly influence the transformation of DBNPA to MBNPA.

The identity of TP2 was confirmed to be 2,2-dibromopropanediamide (Table 2; Text S8) by retention time and fragmentation spectra alignment with a commercially available standard. 2,2-Dibromopropanediamide is formed as result of the hydration of the nitrile group of DBNPA to an amide group. 2,2-Dibromopropanediamide has not been described before as an environmental TP of DBNPA. However, the industrial production of 2,2-dibromopropanediamide from DBNPA as well as the simultaneous use of DBNPA and 2,2-dibromopropanediamide for antimicrobial purposes has been described in various patents (e.g. Gartner and Carsten, 2015). TP2-2,2-Dibromopropanediamide was only present in the DG-samples in the UP-matrix at 1 h (Table 2; Fig. 2D). However, TP2-2,2-dibromopropanediamide appears in the DG-CW-sample and D-CW-sample after 48 h and is present in all DBNPA-containing samples after 96 h. The presence of TP2-2,2-dibromopropanediamide in the D-samples shows that it is a TP of DBNPA itself, but its earlier presence in the DG-samples (Fig. 2D) indicates that glutaraldehyde increases the nitrile to amide conversion rate.

Features corresponding to dibromoacetonitrile and bromoacetonitrile were also identified, similar to what was observed by Exner et al. (1975), Blanchard et al. (1987) and Sumner and Plata (2018). Dibromoacetonitrile is three times more toxic than DBNPA to aquatic fauna, such as *Pimephales promelas* (Mayes et al., 1985). However, component clustering performed by RAMClustR (Fig. 1) showed very similar elution profiles of bromoacetonitrile and dibromoacetonitrile to those of the parent compounds DBNPA (Fig. S5) and MBNPA (Fig. S6). This led to the conclusion that these were fragments resulting from in-source fragmentation of both DBNPA and MBNPA, and not actual TPs. The comparison with commercially available standards of bromoacetonitrile and dibromoacetonitrile confirmed this. Hence, under the current experimental and analytical conditions, only MBNPA and 2,2-dibromopropanediamide could be detected.

3.2.3. Combined effect of glutaraldehyde and DBNPA

The combination of equal concentrations of glutaraldehyde and DBNPA had a lower toxic effect on the CW microorganisms than the corresponding concentration of DBNPA alone, evidenced by the $BioT_{50}$ of benzoic acid (Fig. 3; Table 1). However, the $BioT_{50}$ for the combination of biocides is higher than the $BioT_{50}$ of glutaraldehyde, implying that there is still an effect of the DBNPA. The increase of the $BioT_{50}$ is mainly due to the increased lag-phase (Table 1). Similar to the experiments in section 3.2.1 and 3.2.2, no abiotic removal of benzoic acid was observed.

One reason for this unexpected low inhibitory effect of the

combination of glutaraldehyde and DBNPA is the influence of glutaraldehyde on the DBNPA transformation process (paragraph 3.2.2). The presence of glutaraldehyde led to a higher production of MBNPA (Fig. 2B; C), which is less toxic than DBNPA and which prevents the formation of the more toxic dibromoacetonitrile (Blanchard et al., 1987). Furthermore, faster production of 2,2-dibromopropanediamide was observed in the presence of glutaraldehyde. In addition, we hypothesize that the antagonistic inhibiting effect on CW microorganisms could be the result of the mutual interaction between DBNPA and glutaraldehyde, resulting in products that are less toxic than DBNPA itself. McLaughlin et al. (2016) described that the aldehyde functional groups of glutaraldehyde can covalently bind with amide groups of chemicals, resulting in the formation of by-products. DBNPA possesses such an amide functional group, and we hypothesize that this moiety could react with the aldehyde groups of glutaraldehyde. The non-target screening combined with the data-processing workflow provided 5 potential products of the reaction between glutaraldehyde and DBNPA, 3 of which were brominated (Table 2).

TP3-mz183 (Text S9; Table 2) has an *m/z* of 183.0760. GenForm (Fig. 1) assigned molecular formula $C_8H_{10}N_2O_3$ to this TP. MetFrag (Fig. 1) was not able to find a compound with a suitable molecular structure in its database, probably due to the poor fragmentation of this TP and the absence of this compounds in the PubChem database. Nevertheless, manual inspection of the temporal behaviour of the peak intensity and presence in different matrices combined with background knowledge on the parent compounds can aid in the tentative identification of TPs.

The peak of TP3-mz183 showed distinct features: an increase in peak intensity over time and a higher peak intensity in the CW-matrix (Fig. 4A). The increasing TP3-mz183 peak intensity (Fig. 4A) shows similarities with the increasing peak intensity of TP1-MBNPA (Fig. 2B; C). This could hint towards the relevance of MBNPA in the formation of TP3-mz183. TP3-mz183 could have formed as result of the interaction of the glutaraldehyde monomer ($C_5H_8O_2$) with the amide group of nitrilopropionamide (NPA) ($C_3H_4N_2O$). NPA was not detected in this study, but is a known TP from DBNPA resulting from the loss of the single bromine atom of MBNPA (Blanchard et al., 1987). Glutaraldehyde might react with NPA by Michael-type addition, as is commonly found in the interaction of glutaraldehyde with proteins (Migneault et al., 2004; Rojas, 2015). A proposed structure of TP3-mz183 and a proposed reaction pathway of DBNPA and glutaraldehyde interaction are displayed in Fig. 5. However, no commercially available standards were available to confirm this hypothetical molecular structure.

TP4-mz263 (Table 2; Fig. 5; Text S10) has a *m/z* of 263.0783. GenForm was not able to assign a molecular formula to TP4-mz263. MetFrag proposed several compounds with molecular formula $C_{11}H_{12}N_4O_4$, but these did not seem related to the structure of parent compounds DBNPA and glutaraldehyde. However, it is known that glutaraldehyde is a crosslinking agent for various chemicals, such as proteins and enzymes containing amide groups (Barbosa et al., 2014). According to its molecular formula, TP4-mz263 could be two NPA molecules crosslinked by glutaraldehyde (Fig. 5; Text S10). However, this is highly speculative. TP4-mz263 is only present above the peak intensity threshold (Text S5) in the CW-matrix after 48 h, with an increasing intensity over time (Fig. 4B). Since this is similar to the transformation of DBNPA towards MBNPA and eventually NPA, this could indicate that the formation of TP4-mz263 is dependent on the transformation of DBNPA.

TP5-mz280, TP6-mz280 and TP7-mz280 (Table 2; Fig. 5; Text S13) are isomers with a *m/z* of 280.0292. The MS/MS of these TPs showed distinct bromine isotope peaks (Text S11), revealing that these are a reaction product containing a single bromine ion. The molecular formula $C_8H_{14}N_3O_3Br$ was proposed by both GenForm and MetFrag. MetFrag did not propose compounds that could be related to the structure of the parent compounds. TP5-mz280, TP6-mz280 and TP7-mz280 contained the distinct fragments *m/z* 241.9929 and *m/z* 161.9429. Fragment 241.9929 was assigned to $C_8H_9BrN_2O_2$, which forms as result of the loss of H_5NO from the precursor ion. Fragment 161.9429 was identified earlier as MBNPA. This could indicate that MBNPA is the backbone of TP5-mz280, TP6-mz280 and TP7-mz280. However, the MS/MS spectrum of the fragment (Fig. S7) was different to that of MBNPA itself (Text S7), leaving room for discussion about the actual structure of this fragment. The combined presence of fragment ions 161.9429 and 241.9929 could indicate a structure similar to TP3-mz183, but with the one bromine containing MBNPA instead of the debrominated NPA as backbone of the compound (Fig. 5).

The contribution of TP3 - TP7 to the antagonistic toxic effect of the combination of DBNPA and glutaraldehyde could be substantial, since the peak intensity of for instance TP3mz183 (Fig. 4A) is in the same range as the peak intensity of DBNPA (Fig. 2A) and MBNPA (Fig. 2B; C). TP3-TP7 lower the toxic effect of DBNPA to CW microorganisms, probably because these TPs are less toxic than DBNPA itself. In addition, the formation of these TPs might prevent the formation of more toxic DBNPA transformation products, such as dibromoacetonitrile. Although the toxic effect of DBNPA was partially mitigated, the mixture of these TPs and parent compounds still negatively influenced the biodegradation of benzoic acid by the CW microorganisms. Hence, the combination of DBNPA and glutaraldehyde could lower the pre-treatment efficiency of the CW. To further elucidate the impact of these TPs,

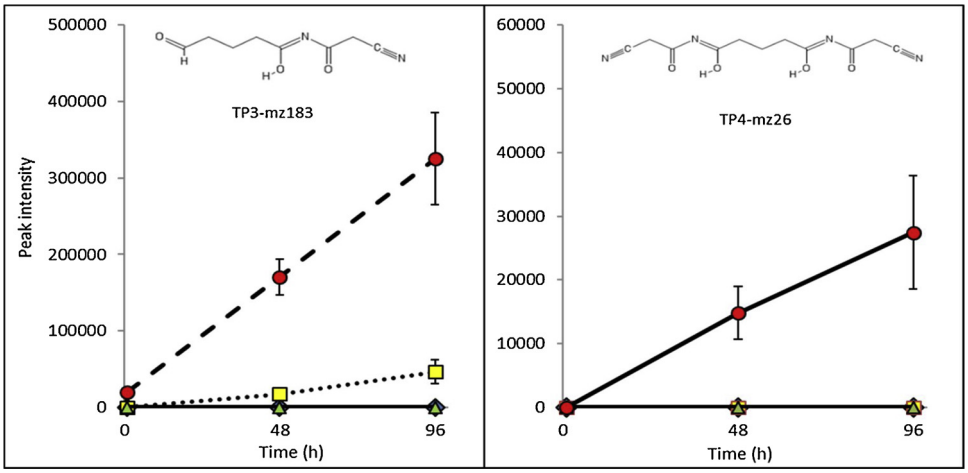

Fig. 4. The peak intensity of TP3-mz183 (A) and TP4-mz263 (B) over time. A distinction is made between samples in: UP-water (blue diamond); UP-water + glutaraldehyde (yellow square); CW-matrix (green triangle); CW-matrix + glutaraldehyde (red circle).

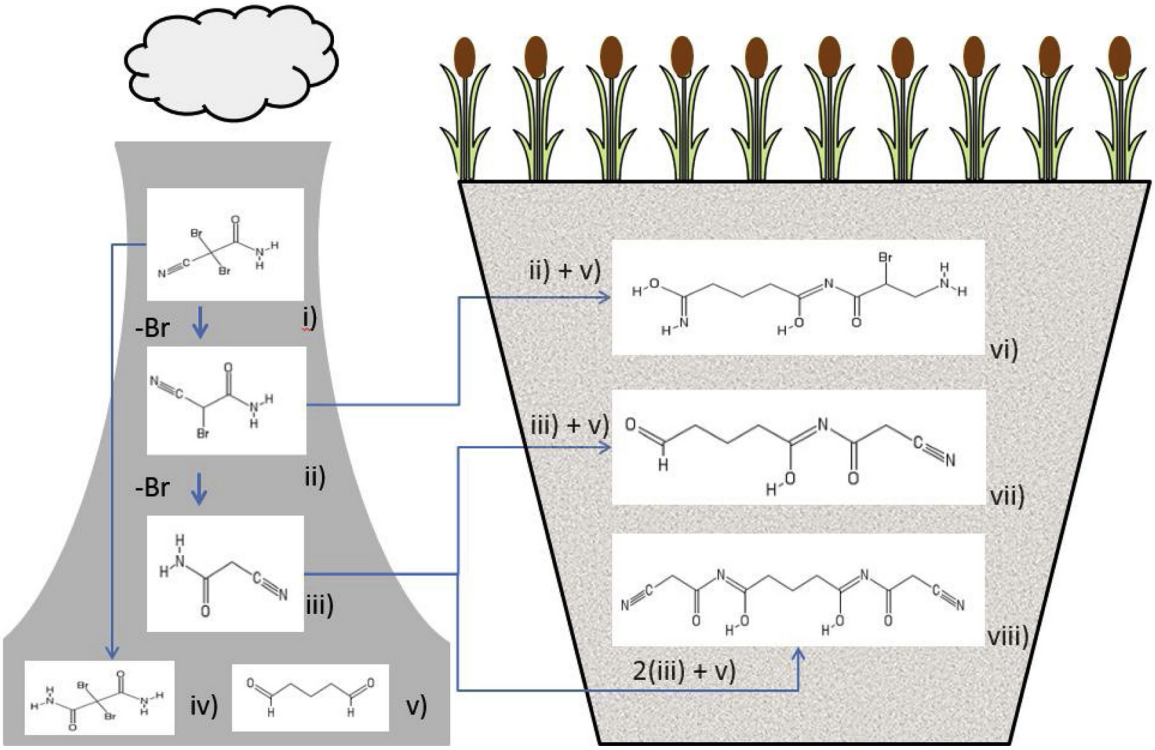

Fig. 5. Proposed chemical reaction pathway of DBNPA, its transformation products and glutaraldehyde. i) DBNPA; ii) TP1-MBNPA; iii) NPA; iv) TP2-2,2-dibromopropanediamide; v) glutaraldehyde; vi) TP5mz280 / TP6mz280 / TP7mz280; vii) TP3mz183; vii) TP4-mz263.

the toxicity of these TPs, their fate in the CW, and their long-term effect on the functioning of the CW should be studied.

4. Conclusions

In this study, the impact of different concentrations of the biocides DBNPA and glutaraldehyde on the biodegradation by constructed wetland microorganisms was tested, and it was shown that glutaraldehyde and/or DBNPA can negatively impact the microbial activity of constructed wetland microorganisms, resulting in a lower biodegradation efficiency. This can severely limit the suitability of a constructed wetland for the pre-treatment of cooling tower water prior to physico-chemical desalination. However, both biocides can be removed abiotically, and a constructed wetland design in which this abiotic removal is promoted could mitigate the negative impact of the biocides on the biodegradation.

Surprisingly, the negative impact of the combination of DBNPA and glutaraldehyde on the biodegradation capacity was lower than that of DBNPA alone. This is the first study that shows that the simultaneous use of DBNPA and glutaraldehyde results in antagonistic toxic effects, and we provide evidence for the mechanisms behind this antagonistic toxic effect by using non-target screening. The non-target screening revealed that the presence of glutaraldehyde resulted in an increased formation of the less toxic DBNPA transformation product MBNPA and quicker production of the newly discovered environmental DBNPA transformation product 2,2-dibromopropanediamide. The formation of these direct transformation products might prevent the formation of other more toxic DBNPA transformation products. Furthermore, new brominated and non-brominated products resulting from the interaction between the DBNPA and glutaraldehyde were tentatively identified. The formation of these new products was influenced by interactions with the constructed wetland matrix and was positively correlated with the formation of direct DBNPA transformation products. The interaction products are likely to be less toxic than DBNPA.

Declaration of Competing Interest

The authors declare that there are no conflicts of interest.

Acknowledgements

This research is financed by the Netherlands Organisation for Scientific Research (NWO), which is partly funded by the Ministry of Economic Affairs and Climate Policy, and co-financed by the Netherlands Ministry of Infrastructure and Water Management and partners of the Dutch Water Nexus consortium: http://waternexus.nl/. Hans Beijleveld, Livio Carlucci, Katja Grolle, Dagmar Kuiper, Thomas Verouden, Tamara de Groot, Myrthe Dullaart, Olaf de Haan, Jules Koppen, Evelien van Maarseveen, Cas Verbeek and Tamara de Groot are acknowledged for their experimental support. Laura Piai, Koen van Gijn and Andrea Aldas Vargas and anonymous reviewers are acknowledged for critically reviewing the manuscript.

Appendix A. Supplementary data

Supplementary material related to this article can be found, in the online version, at doi:https://doi.org/10.1016/j.jhazmat.2019.121661.

References

Albergamo, V., Helmus, R., de Voogt, P., 2018. Direct injection analysis of polar micropollutants in natural drinking water sources with biphenyl liquid chromatography coupled to high-resolution time-of-flight mass spectrometry. J. Chromatogr. A 1569, 53–61.

Altman, S.J., Jensen, R.P., Cappelle, M.A., Sanchez, A.L., Everett, R.L., Anderson, H.L., McGrath, L.K., 2012. Membrane treatment of side-stream cooling tower water for reduction of water usage. Desalination 285, 177–183.

Avila, C., Bayona, J.M., Martin, I., Salas, J.J., Garcia, J., 2015. Emerging organic contaminant removal in a full-scale hybrid constructed wetland system for wastewater treatment and reuse. Ecol. Eng. 80, 108–116.

Barbosa, O., Ortiz, C., Berenguer-Murcia, A., Torres, R., Rodrigues, R.C., Fernandez-Lafuente, R., 2014. Glutaraldehyde in bio-catalysts design: a useful crosslinker and a versatile tool in enzyme immobilization. RSC Adv. 4, 1583–1600.

Blanchard, F.A., Gonsior, S.J., Hopkins, D.L., 1987. 2,2-dibromo-3-nitrilopropionamide (DBNPA) chemical degradation in natural waters: experimental evaluation and modelling of competitive pathways. Water Res. 21, 801–807.

Bertheas, U., Majamaa, K., Arzu, A., Pahnke, R., 2009. Use of DBNPA to control biofouling in RO systems. Desalin. Water Treat. 3, 175–178.

Campa, M.F., Techtmann, S.M., Gibson, C.M., Zhu, X., Patterson, M., Garcia de Matos Amaral, A., Ulrich, N., Campagna, S.R., Grant, C.J., Lamendella, R., Hazen, T.C., 2018. Impacts of glutaraldehyde on microbial community structure and degradation potential in streams impacted by hydraulic fracturing. Environ. Sci. Technol. 52, 5989–5999.

Exner, J.H., Burk, G.A., Kyriacou, D., 1973. Rates and products of decomposition of 2,2-dibromo-3-nitrilopropionamide. J. Agric. Food Chem. 21, 838–842.

Faber, A.H., Annvelink, M., Gilissen, H.K., Schot, P., van Rijswick, M., de Voogt, P., van Wezel, A., 2017. How to adapt chemical risk assessment for unconventional hydrocarbon extraction related to the water system. Rev. Environ. Contam. Toxicol. 246, 1–32.

FAO, 2016. AQUASTAT Main Database. Food and Agriculture Organization of the United Nations (FAO) Website accessed on [27/01/2017 10:25].

Ganzer, G., Summerfield, J., Freid, M., Soost, J., Regginni, G., 2002. The Use of glutaraldehyde/DBNPA Combination Treatment Program for Effective Control of Microbial Growth in Cooling Water Systems, Corrosion 2002. NACE International.

Garcia, J., Rousseau, D.P., Morato, J., Lesage, E., Matamoros, V., Bayona, J.M., 2010. Contaminant removal processes in subsurface-flow constructed wetlands: a review. Crit. Rev. Environ. Sci. Technol. 40, 561–661.

Gartner, C.D., Carsten, D. (2015). US Patent No. US 9,221,748 B2 : Process for preparing 2,2-dibromomalonamide.

Groot, C., van den Broek, W., Loewenberg, J., Koeman-Stein, N., Heidekamp, M., de Schepper, W., 2015. Mild desalination of various raw water streams. Water Sci. Technol. 72, 371–376.

Haanstra, L., Doelman, P., Voshaar, J.O., 1985. The use of sigmoidal dose response curves in soil ecotoxicological research. Plant Soil 84, 293–297.

He, Y., Nurul, S., Schmitt, H., Sutton, N.B., Murk, T.A.J., Blokland, M.H., Rijnaarts, H.H.M., Langenhoff, A.A.M., 2018. Evaluation of attenuation of pharmaceuticals, toxic potency, and antibiotic resistance genes in constructed wetlands treating wastewater effluents. Sci. Total Environ. 631-632, 1572–1581.

Helmus, R., 2018. 'patRoon'. http://github.com/rhelmus.

Hijosa-Valsero, M., Reyes-Contreras, C., Dominguez, C., Becares, E., Bayona, J.M., 2016. Behaviour of pharmaceuticals and personal care products in constructed wetland compartments: influent, effluent, pore water, substrate and plant roots. Chemosphere 145, 508–517.

Imfeld, G., Braeckevelt, M., Kuschk, P., Richnow, H.H., 2009. Monitoring and assessing processes of organic chemicals removal in constructed wetlands. Chemosphere 74 (3), 349–362.

IPCS INCHEM, 2005. International programme on chemical safety. Screening Information Data Set (SIDS) Glutaraldehyde. . http://www.inchem.org/documents/sids/sids/111308.pdf.

Jasper, J.T., Jones, Z.L., Sharp, J.O., Sedlak, D.L., 2014. Biotransformation of trace organic contaminants in open-water unit process treatment wetlands. Environ. Sci. Technol. 48, 5136–5144.

Kahrilas, G.A., Blotevogel, J., Stewart, P.S., Borch, T., 2015. Biocides in hydraulic fracturing fluids: a critical review of their usage, mobility, degradation, and toxicity. Environ. Sci. Technol. 49, 16–32.

Klaine, S.J., Cobb, G.P., Dickerson, R.L., Dixon, K.R., Kendall, R.J., Smith, E.E., Solomon, K.R., 1996. An ecological risk assessment for the use of the biocide dibromonitrilopropionamide (DBNPA), in industrial cooling systems. Environ. Toxicol. Chem. 15, 21–30.

Leung, H., 2001a. Ecotoxicology of glutaraldehyde: review of environmental fate and effects studies. Ecotoxicol. Environ. Saf. 49 (1), 26–39.

Leung, H., 2001b. Aerobic and anaerobic metabolism of glutaraldehyde in a river water–sediment system. Arch. Environ. Contam. Toxicol. 41 (3), 267–273.

Löwenberg, J., Baum, J.A., Zimmermann, Y., Groot, C., van den Broek, W., Wintgens, T., 2015. Comparison of pre-treatment technologies towards improving reverse osmosis desalination of cooling tower blow down. Desalination 357, 140–149.

Macknick, J., Newmark, R., Heath, G., Hallett, K., 2012. Operational water consumption and withdrawal factors for electricity generating technologies: a review of existing literature. Environ. Res. Lett. 7 (4), 045802.

Mayes, M.A., Blanchard, F.A., Hopkins, D.L., Takahashi, I.T., 1985. Static acute toxicity of dibromonitrilopropionamide and selected degradation products to the fathead minnow (*Pimephales promelas Rafinesque*). Environ. Toxicol. Chem. 4, 823–830.

McLaughlin, M.C., Borch, T., Blotevogel, J., 2016. Spills of hydraulic fracturing chemicals on agricultural topsoil: biodegradation, sorption, and co-contaminant interactions. Environ. Sci. Technol. 50, 6071–6078.

Migneault, I., Dartiguenave, C., Bertrand, M.J., Waldron, K.C., 2004. Glutaraldehyde: behavior in aqueous solution, reaction with proteins, and application to enzyme crosslinking. BioTechniques 37 (5), 790–806.

Oetjen, K., Giddings, C.G.S., McLaughlin, M., Nell, M., Blotevogel, J., Helbling, D.E., Mueller, D., Higgins, C.P., 2017. Emerging analytical methods for the characterization and quantification of organic contaminants in flowback and produced water. Trends Environ. Anal. Chem. 15, 12–23.

Pan, S., Snyder, S.W., Packman, A.I., Lin, Y.J., Chiang, P., 2018. Cooling water use in thermoelectric power generation and its associated challenges for addressing water-energy-nexus. Water-Energy Nexus 1, 26–41.

R Core Team, 2013. R: a Language and Environment for Statistical Computing. URL. R Foundation for Statistical Computing, Vienna, Austria. http://www.R-project.org/.

Rogers, J.D., Ferrer, I., Tummings, S.S., Bielefeldt, A.R., Ryan, J.N., 2017. Inhibition of biodegradation of hydraulic fracturing compounds by glutaraldehyde: groundwater column and microcosm experiments. Environ. Sci. Technol. 51 (17), 10251–10261.

Rojas, J., 2015. Improved polymer functionality by cross-linking with glutaraldehyde to achieve controlled drug release. Excipient Appl. Formul. Des. Drug Deliv. 569–588.

Russell, A.D., 2003. Similarities and differences in the responses of microorganisms to biocides. J. Antimicrob. Chemother. 52, 750–763.

Schymanski, E.L., Jeon, J., Gulde, R., Fenner, K., Ruff, M., Singer, H.P., Hollender, J., 2014. Identifying small molecules via high resolution mass spectrometry: communicating confidence. Environ. Sci. Technol. Lett. 48, 2097–2098.

Sumner, A.J., Plata, D.L., 2018. Halogenation chemistry of hydraulic fracturing additives under highly saline simulated subsurface conditions. Environ. Sci. Technol. 52, 9097–9107.

Vikram, A., Lipus, D., Bibby, K., 2014. Produced water exposure alters bacterial response to biocides. Environ. Sci. Technol. 48, 13001–13009.

Vikram, A., Bomberger, J.M., Bibby, K.J., 2015. Efflux as a glutaraldehyde resistance mechanism in *Pseudomonas fluorescens* and *Pseudomonas aeruginosa* biofilms. Antimicrob. Agents Chemother. 59 (6), 3433–3440.

Wagner, T.V., Parsons, J.R., Rijnaarts, H.H.M., de Voogt, P., Langenhoff, A.A.M., 2018. A review on the removal of conditioning chemicals from cooling tower water in constructed wetlands. Crit. Rev. Environ. Sci. Technol. 48, 1094–1125.

Wagner, T.V., Parsons, J.R., Rijnaarts, H.H.M., de Voogt, P., Langenhoff, A.A.M., 2020. Benzotriazole removal mechanisms in pilot-scale constructed wetlands treating cooling tower water. J. Hazard. Mater. 384. https://doi.org/10.1016/j.jhazmat.2019.121314.

de Wilt, A., He, Y., Sutton, N., Langenhoff, A., Rijnaarts, H., 2018. Sorption and biodegradation of six pharmaceutically active compounds under four different redox conditions. Chemosphere 193, 811–819.

Zhang, C., Zhong, L., Fu, X., Wang, J., Wu, Z., 2016. Revealing water stress by the thermal power industry in China based on a high spatial resolution water withdrawal and consumption inventory. Environ. Sci. Technol. 50, 1642–1652.